This is a peer-reviewed, accepted author manuscript of the following article: Hashem, A., Nasr, M. F., Fletcher, A. J., & Mohamed, L. A. (2020). Aminated acrylic fabric waste derived sorbent for Cd(II) ion removal from aqueous solutions: mechanism, equilibria and kinetics. *Gels*. https://doi.org/10.1007/s10924-020-01863-z

Aminated acrylic fabric waste derived sorbent for Cd(II) ion removal from aqueous solutions: mechanism, equilibria and kinetics

A. Hashem[a]*, M.F. Nasr[a], A. J. Fletcher[b], and Latifa A. Mohamed[c]

[a] National Research Center, Textile Research Division, Dokki, Cairo, Egypt.

[b] Department of Chemical and Process Engineering, University of Strathclyde, 75 Montrose Street, Glasgow, G1 1XJ, UK.

[c] Microbial Chemistry Department, National Research Center, Dokki, Cairo, Egypt.

*Author to whom all correspondence should be addressed. E-mail: alihashem2000@yahoo.com.

Abstract

An aminated acrylic fiber waste (AAFW) has been utilized as an adsorbent material for the removal of Cd(II) ions from aqueous solution after treatment of acrylic fiber waste (AFW) with hydroxylamine hydrochloride under basic conditions, and characterized for surface chemistry, surface morphology and textural properties. The ability of this sorbent to adsorb Cd(II) ions was examined via batch adsorption methods, studying the effect of pH, sorbent and sorbate concentrations, as well as contact time. Results obtained confirm that this sorbent was effective for Cd(II) ion adsorption, with uptakes promoted by high active site density, however, the adsorption process is independent of sorbent surface area.

The values obtained exceed those previously reported within the literature. Isotherm analysis using arrange of two- and three- parameter models, evaluated using non-linear regression methods with error analysis, showed that the Langmuir isotherm model most appropriately described the experimental data obtained, indicating mono layer adsorption occurs. Kinetic analysis using arrange of models in their non-linear forms provided mechanistic information, showing that pseudo - second-order behavior is involved. The synthesized aminated acrylic fiber waste derived sorbents offer significant potential for the removal of Cd (II) ions from aqueous solution through a mechanism of chelation between the electron- donating oxygen-and nitrogen-containing groups in the sorbent and the electron-accepting Cd(II)ions.

Keywords: Amination; Isotherm models; kinetic models; FTIR; BET; SEM

1. Introduction

Wastewater adulteration with significant levels of metal species is a genuine natural issue, with high potential impact as a consequence of the hazardous nature of such contaminants; this includes danger towards marine organisms, non-biodegradability, bioaccumulation, and is compounded by the high capital expense of removing such pollutants from wastewater. High levels of metals, e.g. cadmium, lead, mercury, copper, nickel and zinc, are found in mechanical wastewater releases as a consequence of highly polluting processes including mining and metallurgical practices, electroplating, and the creation of synthetic substances, for example, dyes, composts, and pesticides. This pollution of natural resources has significant negative impacts on flora and fauna, exacerbated by their ubiquitous presence in developed life styles [1, 2].

Cadmium has been previously identified as an important heavy metal pollutant , and has been proven to exhibit high levels of toxicity even at very low concentrations, resulting in a range of biological impacts in living beings, including humans[3]. With significant discharges from a range of industries, including mining, oil refineries, metal plating, batteries manufacture, alloy industries, smelting, phosphate fertilizers and pigments [4-6], high levels have been observed that require remediation [7]. Traditional techniques used for

removal of heavy metal pollutants from industrial wastewater effluents include separation with membranes [8],ion exchange [9], electrolysis [10], chemical precipitation [11] and adsorption onto activated carbons[12, 13]; however, most of these techniques suffer from practical drawbacks, such as problematic disposal of waste materials, as well as the high capital needed for several operations and processes. By comparison, adsorption processes are the most common and effective techniques applied for removing heavy metal pollutants from their aqueous solutions [14, 15], and activated carbons can be relatively inexpensive materials, especially if they are derived from waste components. Activated carbons have been widely used as sorbents in wastewater treatment systems; however, they can be unsuitable for developing countries due to high operational costs [16-18].

In order to enhance adsorption of metal species, chelating resins and polymers have been used to treat wastewater and recover metal ions from a wide range of sources [19, 20] and the preparation of chelating fibrous materials through the introduction of functional groups into the chemical structure of industrial fibers is a good approach to the production of new high-efficiency metal sorbents [21, 22]. Instead of simply exchanging ions, the process of chelation should be highly selective. By utilizing waste materials, as has been routinely done for activated carbons, this allows for high performance, low-cost sorbents to be created. With a

combination of low-cost, ease of modification and good stability in aqueous media, polyacrylonitrile fiber is the most used for this purpose [23] and is utilized here.

In this study, aminated acrylic fiber waste (AAFW) was used to synthesize a new sorbent for the removal of Cd(II) from aqueous media. The preparation of these sorbents was achieved by the reaction of acrylic fiber waste (AFW) with hydroxylamine hydrochloride under alkaline conditions. The obtained product was characterized to investigate the surface functional groups, morphology, and surface area. The effects of pH, initial concentration of Cd(II), and exposure time were also studied providing information on isothermal equilibria, sorption kinetics and mechanism of sorption.

2 .Materials and methods

The acrylic fiber wastes used in this study are supplied from the fiber production line of the A ksa Egypt Acrylic Fiber Company, Borg El-Arab Alexandria, Egypt, in the form of acrylic soft waste. All reagents used in this study: cadmium acetate, sodium hydroxide, ethylenediaminetetraacetic acid, nitric acid, sodium carbonate, hydrochloric acid, acetone, and ethyl alcohol, were laboratory grade chemicals supplied by Merck, Germany.

2.1. Preparation of aminated acrylic fiber waste derived sorbents

4.5 g of hydroxylamine hydrochloride was solubilized in 30 mL of a 5:1 methanol-water mixture to produce a free solution of hydroxylamine; with the hydrochloride species fully neutralized using 0.1 M sodium hydroxide solution. 3 g of the acrylic fiber waste was kepts welling in10 mL of methanol overnight before addition of the previously-prepared free hydroxylamine solution in a flask fitted with condenser. The aminated acrylic fiber waste (Scheme1) was prepared by refluxing at 100 °C for 8 h, prior to filtering and washing thoroughly with sufficient distilled water to ensure that any unreacted hydroxylamine was removed, and subsequent drying at 60 °C for 3 h.

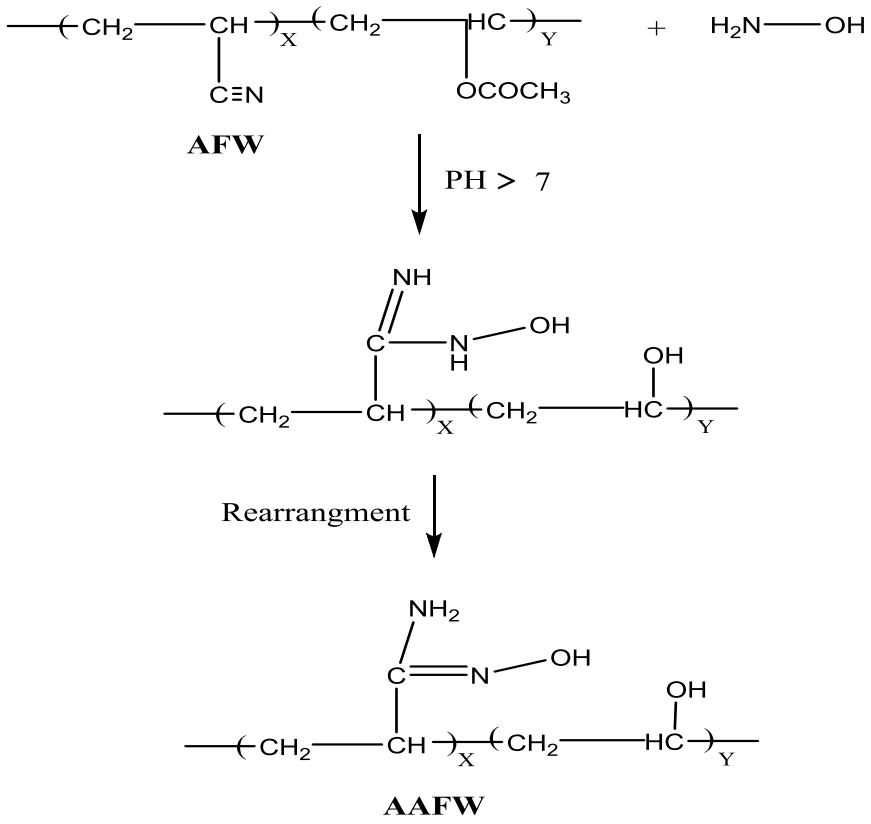

Scheme 1: Preparation of aminated acrylic fiber waste sorbent (AAFW) from acrylic fiber waste (AFW).

2.2. Batch Adsorption Studies

0.03 g of adsorbent was added to 100 mL of a Cd(II) ion solution (100–1000 mg L^{-1}), prepared using cadmium acetate, in a 125 mL Erlenmeyer flask. 0.1 M nitric acid or 0.1 M sodium hydroxide was added drop wise to adjust pH values to the required value and the mixture shaken at 30 °C, at a constant speed of 150 rpm, for a pre-defined period, before filtering. The concentration of Cd(II) ions was measured before and after adsorption, using direct titration with a standard solution of ethylenediaminetetraacetic acid (EDTA, 0.5 mM).

The amount of Cd(II) adsorbed at equilibrium, qe (mgg^{-1}) was calculated using:

$$q_e = \frac{V(C_o - C_e)}{W} \quad (1)$$

While the percentage removal was calculated via:

$$\text{Removal } \% = \frac{(C_o - C_e)}{C_o} \cdot 100 \quad (2)$$

Where C_o and C_e (mg L-1) are the initial metal concentration and metal concentration at equilibrium, respectively; W(g) is the weight of adsorbent used, and V is the volume of Cd (II) solution (0.1 L).

2.3. Sorbent characterization

FT-IR-spectroscopy

The aminated acrylic fabric waste, hereon denoted AAFW, and AAFW loaded with Cd(II) post-adsorption were characterized using Fourier Trans forminfrared spectroscopy (FTIR) to assign vibrational frequencies of different functional groups present in the parent adsorbent structure, as well as to determine the nature of any bonds formed between Cd (II) ions and the adsorbent surface. FTIR spectra of KBr discs containing ~2-10 mg of sample in ~300 mg of KBr were recorded using a Perkin–Elmer Spectrum1000 spectrophotometer (USA) over a wavelength range of 4000–400 cm^{-1} at a scan interval of 1 cm^{-1} over 120 scans.

Scanning electron microscopy (SEM)

A sample of each sorbent was coated with chromium on carbon tape and then imaged using a TESCAN CE VEGA 3 SBU (117-0195- Czech Republic) scanning electron microscope (SEM). Images were recorded using 2000x magnification and the technique provided information on the morphology of the parent fibers and the synthesized AAFW sorbent.

Energy–dispersive X-ray analysis (EDX)

Energy-dispersive X-ray (EDX) patterns were recorded using adispersive X-ray fluorescence (EDX) spectrometer (Oxford Instruments) attached to a scanning

electron microscope (JEOL-JSM-5600- Czech Republic).The test was performed on post-adsorption AAFW samples to determine the presence or absence of Cd(II) ions using the characteristic band of cadmium metal for confirmation.

BET surface area measurement

The textural characteristics of AAFW were determined via nitrogen adsorption using an Auto sorbI assembly. Analysis was conducted using oxygen-free nitrogen gas (Nova 2000, Quanta Chrome Instrument, Beach, USA) at-196 °C, and the isothermal data obtained analyzed using the Brunauer-Emmet-Teller method. Meso pore volume, external surface area, and meso pore surface area were determined using the t-plot method, while the Barrett-Joyner-Halenda technique was used to calculate the average pore width and obtain the pore size distribution.

Determination of point of zero charge (pHpzc)

A solid addition method was used to evaluate the pH at the point of zero charge pHpzc for AAFW. Typically, 100 mL of 0.01 N NaCl was added to a series of conical flasks and the pH adjusted using an aqueous solution of 0.01 NHCl and 0.01 N NaOH to adjust the pH within the range 2 to12. The initial pH was recorded after a constant pH value was attained; thereafter,~100 m g of the AAFW was dispersed in the conical flasks and incubated for 24 h to obtain the final pH. The

161 initial and final pH was plotted, with the point of intersection of the plots denoting
162 the pHpzc of the adsorbent.

163 **2.4. Error analysis**

164 Error functions were defined to evaluate the fit of the selected isotherm models
165 (Langmuir, Freundlich, Temkin, Redlich-Peterson, Toth and Khan, and Sips) to the
166 experimental equilibrium data. The common error functions used here to optimize
167 the isotherm parameters were: average relative error (ARE), average percentage
168 error (APE %), hybrid fractional error function (HYBRID), a determinant of the
169 quality of the fit (χ^2), and normalized standard deviation ($\Delta q\%$)[24-28]. Data
170 obtained for isothermal studies and the associated fits are presented in Table 1(see
171 supporting information).

172 **3. Results and Discussion**

173 **3.1. Characterization of sorbent material (AAFW)**

174 **3.1.1. FT-IR of AAFW**

175 The FT-IR spectra of AFW, AAFW and AAFW loaded with Cd(II) ions are
176 illustrated in Figs.1(a)–(c), respectively. The difference in the finger print peaks of
177 the spectra are evident, and confirm the occurrence of both amination and
178 adsorption processes. Fig. 1(a) shows bands at 3746 cm^{-1} and 2928 cm^{-1}, which are
179 characteristic of O-H stretching and C-H stretching of AFW, respectively. The

sharp peak at 2244 cm^{-1} is attributed to C≡N stretching of the nitrile group in the polymer chain of AFW. The bands at 1728 cm^{-1} are attributed to C=O stretching of ester (vinyl acetate) of the AFW chain. The peak at 1448 cm^{-1} is due to C-H bending of methyl esters. Fig. 1(b) shows the disappearance of the cyanide group of AFW due to the conversion of AFW to AAFW, by reaction with free hydroxylamine solution [29]. Fig.1 (b) also exhibits a broad peak at 3207 cm−1 due to hydrogen bonding between the–OH group of AFW and amine groups in the chains of AAFW. The peaks at 2923 cm^{-1} and 1641 cm^{-1} are attributed to C-H stretching, and N-H bending of amine in AAFW. The peaks at 1381 cm^{-1} and 928 cm^{-1} are due to C-H bending and C-C bending of AAFW. Fig.1(c) shows a small shift in the absorbance peak for Cd (II)- loaded AAFW compared with that in AFW (a), and AAFW (b). The broad band observed at 3207 cm^{-1} is shifted to 3247 cm^{-1}. The peaks at 2923 and 1641 cm^{-1} are shifted to 2921 and 1642 cm^{-1}, respectively. The peak observed at 1381 cm^{-1} is shifted to 1385 cm^{-1}, indicating strengthening of the relevant bonds.

3.1.2. Morphological characterization of adsorbent by SEM

Fig.2(a) shows the SEM image obtained for AAFW, and the morphology can be seen to be disordered, revealing an agglomerated material with several types of pores. There are no significant changes in the morphology after adsorption of Cd(II), as shown in Fig.2(b), indicating that AAFW is a robust sorbent with

favorable potential for commercialization. The EDX spectra of Cd(II)-loaded AAFW is presented in the chart of Fig.2(c). The presence of sharp peaks cores pending to elemental Cd confirms adsorption of Cd (II) onto AAFW surface.

3.1.3. Surface area characterization of adsorbent by BET

The textural characteristics of the AAFW show a very low BET surface area of 0.1 $m^2 g^{-1}$ with a total pore volume of 3 x 10^{-3} cm3 g^{-1}, and an average pore width of 109 nm. The low surface area is as expected, due to the nature of the prepared aminated acrylic fibers, which is unaffected by conversion to AAFW. The average pore width is in the macro pore region [30, 31], which is beneficial for mass transport, particularly in aqueous systems, enhancing contact with and adsorption of Cd (II).

3.2. Factors affecting Cd(II) adsorption onto AAFW

Several factors are known to influence the adsorption of heavy metals, including adsorbent dose, pH, adsorptive concentration and contact time. These four parameters were investigated to understand their impact on the adsorption behavior of AAFW.

3.2.1. Point of zero charge (pHpzc) and the effect of pH

Fig. 3 shows the data obtained for determination of the pHpzc for the surface of the AAFW sorbent, defining the pH at which the surface of has a neutral charge. The

219 pH_{pzc} of AAFW was determined as 8.0 indicating that the surface of AAFW is
220 alkaline in nature. When the pH value of the solution is higher than pHpzc, the
221 surface charge of the sorbent will be negative and favors the binding of cations.
222 When the pH value of the solution is lower than the pH_{pzc}, the surface charge of the
223 sorbent will be positive and, therefore, the adsorption of cations is unfavorable
224 [32]. Figure 3 presents the results of studies in to the effect of pH on the adsorption
225 of Cd (II) ions by AAFW, in the range pH2–7, and an initial Cd(II) ion
226 concentration of 300 mg L^{-1}. The adsorption of Cd(II) increased from 0 to
227 80.5 mg g^{-1} with increasing pH, up to pH 6, before decreasing with a further
228 increase of pH within the range studied. At high acidity (e.g. pH 2), the AAFW
229 surface will be completely covered with H_3O^+ ions, and the Cd (II) ions would be
230 unable to compete with them for adsorption sites (q_e=0). With the increase in pH
231 towards more neutral values ,the competing effect of H_3O^+ decreases and the
232 positively charged Cd(II) ions would adsorb on the free binding sites of the
233 adsorbents indicating a maximum value at pH6. After this point, the uptake
234 decreases again, as active sites are less available on the adsorbent, and equilibrium
235 is established between the Cd (II) ions on the adsorbent and in solution [33].

236 The results indicate that the optimum pH for AAFW to adsorb Cd(II) is6.0, as
237 shown in Fig.9(a), which is lower than the pH_{pzc}, which results in the sorbent
238 surface being predominantly positive, which may lead to electrostatic repulsion

239 between the Cd(II) ions and the positively charged surface [34]. The positive
240 charge of AAFW can be attributed to the character of the nitrogen atoms in the
241 amine groups present on the surface of the polyacrylonitrile fiber, as a consequence
242 of the reaction with free hydroxylamine. It is possible that metal complexes form
243 between the Cd(II) ions and the basic nitrogen of the amine functionalities. This
244 metal complexation may occur in tandem with interactions between the metal ions
245 and the oxygen atoms in the hydroxyl groups on the AAFW, and this may be
246 significant in enhancing adsorption.

247 **3.2.2. Effect of adsorbent dose**

248 Previous studies, including works on meal ion removal, have report an influence
249 from the amount of adsorbent used within an adsorption system. Consequently, the
250 effect of adsorbent dose, in the range 0.3–10 g L^{-1}, on the adsorption capacity of
251 AAFW from a Cd (II) ion solution, of initial concentration 300 mg L^{-1}, was studied
252 at the previously determined pH value for maximal adsorption (pH6). As can be
253 seen from Figure5, the adsorption capacity (q_e) of Cd(II) ions, per gram of
254 adsorbent (mg g^{-1}), decreased from 89.5 to 15mg g^{-1} with increasing adsorbent
255 dose, up to 8 g L^{-1}, where after a plateau is observed. The decrease in adsorption
256 capacity with increasing adsorbent dose, while counterintuitive, can be attributed
257 to the relative number of unsaturated adsorption sites, which increases as more
258 mass is added, thereby decreasing the relative uptake per unit mass. There may

also be effects from the overlap of adsorption sites and overcrowding of adsorbent particles, which has been observed previously for metal ion recovery [33].

3.2.3. Effect of contact time

Contact time is also known to affect adsorption uptakes, as insufficient time prevents equilibrium being established. The effect of contact time on the Cd(II) ion adsorption capacity of AAFW, at an initial adsorptive concentration of 300 mg L^{-1}, is shown in Figure 6. As expected, the adsorption capacity of AAFW increased with increasing contact time, with equilibrium established at 90 min, after which the uptake plateaus with no further enhancement in capacity. It is imperative, for applications of such technologies, that the equilibrium time is short, which is the case here.

3.3. Isothermal analysis of Cd(II) ion adsorption on AAFW

Isothermal data provides information on the final uptake capacity of sorbents and it is evident from the data presented in Table 2 (see the supporting information) that the AAFW material has a very high affinity for the removal of Cd(II) ions from solution, demonstrating significant improvements on other sorbents previously reported in the literature [35-43]. Additionally, adsorption isotherms are used to describe the thermodynamic equilibrium established between the sorbate quantity on the sorbent surface and the amount of solute in solution over a range of concentrations, not just the final capacity. By studying the approach to capacity, it

279 is possible to more fully understand the processes occurring within these
280 adsorption systems. There have been a number of models, with modifications and
281 combinatorial versions, developed to model such systems and provide insight into
282 the behavior observed during adsorption. These can be categorized, in the main, as
283 two- or three-parameter models, arrange of which have been selected to analyze
284 the data obtained within this study. The chosen models comprising two parameters
285 are Langmuir, Temkin, and Freundlich, and those with three parameters are Sips,
286 Redlich-Peterson(R-P), Toth and Khan. All isothermal data analyzed in this study
287 was obtained for adsorption of Cd(II) ions onto AAFW, at pH6, equilibrated for
288 90 min.

289 **3.3.1. Two-parameter isotherm models**

290 The Langmuir isotherm model [44], which is based on monolayer adsorption with
291 a fixed number of localized sites, refers to homogeneous adsorption, with no
292 interact ions between neighboring adsorbate molecules, and an absence of site to
293 site migration of adsorbate. The non-linear form of the Langmuir isothermis:

294 $$q_e = \frac{K_L C_e}{1+bC_e} \qquad 3$$

295 Where C_e is concentration of Cd (II) ions adsorbed at equilibrium, mg L^{-1}, q_e is
296 amount of Cd (II) ions adsorbed per unit mass of adsorbent (mg g^{-1}), K_L(L g^{-1}) and
297 b(L mg^{-1}) are constants. The ratio b/k_L gives the maximum adsorption capacity

298 (q_{max}) inmg g^{-1}. The essential characteristics of Langmuirian behavior can be
299 expressed in terms of the dimensionless separation factor, R_L, [45] represented by:

300

301 $$R_L = \frac{1}{(1+b \cdot C_0)} \qquad 4$$

302 Where C_o is the initial adsorptive concentration in solution, and b is a constant.
303 The Freundlich isotherm model can be applied to systems that exhibit multi layer
304 adsorption and accounts for surface heterogeneity. This empirical model is based
305 on strongest binding sites being, with a logarithmic decrease in adsorption heats
306 across all surface sites. The logarithmic form of the model is[46]:

$$q_e = K_F \cdot C_e^{1/n} \qquad 5$$

307

308 where C_e and q_e are as defined above, and K_F and n are constants related to
309 adsorption capacity and favorability, respectively.

310 The Temkin isotherm model[47] assumes a linear decrease in the distribution of
311 adsorption heats across all surface sites due to adsorbate/adsorbent interactions.
312 The non-linear Temkin isotherm model is represented by:

$$q_e = \frac{RT}{b_T} \cdot ln(A_T C_e) \qquad 6$$

Where C_e and q_e are as defined above, A_T is the Temkin isotherm constant (L g^{-1}), b_T is a constant related to the heat of adsorption (J mol^{-1}), T is absolute temperature (K) , and R is the universal gas constant.

3.3.2. Three-parameter isotherm models

The Redlich–Peterson isotherm model [48] combines features from both the Freundlich and the Langmuir isotherm models, as a consequence it does not follow ideal monolayer adsorption. The model is empirical in nature and approaches the Henry region at infinite dilution, and reduces to the Freundlich model at high liquid-phase concentrations. The non-linear Redlich–Peterson equation is represented by:

$$q_e = \frac{A \cdot C_e}{1 + B \cdot C_e^g} \qquad 7$$

Where C_e and q_e are as defined above, A(L g^{-1}) and B are constants, and g is an exponent constant hat lies between 1and 0; when g= 1, Eq. (7) reduces to the Langmuir equation, and wheng =0, Eq.(7) reduces to Henry's equation, where A/(1+B) is the Henry's constant.

The Toth isotherm model [49] is another modification of the Langmuir equation and is used to describe heterogeneous adsorption systems; it differs by satisfying both low-and high-end concentration boundaries, as expressed by:

$$q_e = \frac{k_T \cdot C_e}{(a_T + C_e)^{\frac{1}{t}}} \quad (8)$$

Where C_e and q_e are as defined above, K_T is a constant, a_T is the maximum adsorption capacity, and 1/t is the Toth exponent constant. The constant t provides a measure of the heterogeneity of the sample and the model reduces to the Langmuir isotherm model when t is close to unity.

The Sips isotherm model [50], which is a combination of the Langmuir and Freundlich isotherm models, again predicts adsorption on heterogeneous surfaces and can be represented by:

$$q_e = \frac{k_s \cdot C_e^{\beta_1}}{1 + a_s \cdot C_e^{\beta_1}} \quad (9)$$

Where C_e and q_e are as defined above, k_s (L g^{-1}) and(L mg^{-1}) are constants, and β_1 is the Sips model exponent t.While the Sips model becomes the Freundlich isotherm model at low adsorptive concentrations, it also reduces to the Langmuir isotherm model, predicting monolayer formation, at high adsorptive concentrations.

The Khan isotherm model [51] was first proposed to describe the adsorption of aromatics on activated carbons, and is used to predict adsorption in binary systems

from pure adsorption data; however, is also applicable to the system studied here, and is expressed by:

$$q_e = \frac{q_{max} \cdot b_K \cdot C_e}{\left(1 + b_K \cdot C_e\right)^{a_K}} \quad (10)$$

Where C_e and q_e are as defined above, b_k is a constant, a_k is the model exponent, and q_{max} is the maximum adsorption capacity (mg g^{-1}).

3.3.3. Error analysis

To determine the most appropriate equation to model the isothermal data obtained in this study, error functions were used to minimize the error between the experimental data and the prediction from each model by optimizing the variance(R^2). Errors between experimental and isothermal model data were minimized using arrange of error functions (ARE, APE%, HYBRID, χ^2, and $\Delta q\%$), optimized using non-linear regression. An example compare is on between the experimental isothermal data obtained here andthefitsofferedbythedifferenttwo-andthree-parameterisothermmodelsoutlined above are shown in Figure 7; all data across the 6 models and different error functions are presented in Tables3and4.Adsorption reversibility is inferred from the value of R_L, as determined from the Langmuir model, which indicates irreversibility when R_L=0, favorability for $0<R_L<1$, linearity if R_L=1, or unfavorability whenR_L>1. The value of n, as determined from the Freundlich model (Table 3) was 1.76, which satisfies

362 the caveat $0 < n < 10$, and also indicates that adsorption of Cd(II) ions onto AAFW
363 is favorable; however, the value of $1/n < 1$ suggests some minor negative impact
364 on adsorption at low equilibrium concentrations. The maximum adsorption
365 capacity for Cd(II) ions onto AAFW, according to the Langmuir isotherm model,
366 was 253 mg L^{-1}, which, as stated above, compares very favorably with other
367 systems (Table 2).

368 The data presented in Table3 indicates that the fit of the two-parameter isotherm
369 models flows the order: Langmuir> Freundlich> Temkin; whilethethree-parameter
370 isotherm models are ordered :Sips> Toth> Khan> Redlich- Peterson (Table 4); this
371 results in an overall ranking of Langmuir> Sips> Toth> Freundlich> Khan>
372 Temkin> Redlich-Peterson, on this basis of error functions and variance
373 minimization.

374 Consequently, the Langmuir model was deemed the most appropriate to model the
375 adsorption of Cd(II) ions on AAFW, suggesting monolayer adsorption, which is in
376 line with the visual representation of the adsorption isotherm (Figures7 and 8).

377 **3.4. Adsorption kinetics**

378 It is not only important to know the amount of material that will be taken up by a
379 sorbent but, from a commercial application perspective, it is imperative to
380 understand the time required to adsorb a pollutant species, thereby informing

residence times for a designed system. It is possible to model the approach to equilibrium, giving insight into the kinetics of adsorption, which can also provide information on the mechanism of adsorption. Here, three kinetic models were used to model the data obtained for the approach to equilibrium with time for adsorption of Cd(II) onto AAFW, namely pseudo-first-order, pseudo-second-order and intra-particle diffusion; the first two looking at reaction kinetics and the latter focusing on kinetic diffusion..

Pseudo-first-order kinetic processes are usually considered physical adsorption and are diffusion controlled; the non-linear mathematical form of the model [52] is given by:

$$q_t = q_e[1 - \exp(-k_1 t)] \qquad 11$$

Where q_t is the amount of Cd (II) ions adsorbed (mg g^{-1}) at time t (min), q_e is the amount of Cd (II) ions adsorbed (mg g^{-1}) at equilibrium, and k_1 is the rate constant of adsorption (min^{-1}).

The pseudo- second order kinetic model [53], which is similar in basis to the pseudo-first order equation except the adsorption of metal ions is controlled by a second order rate equation, can be expressed by:

$$q_t = \frac{k_2 q_e^{2} t}{(1 + k_2 k_e t)} \qquad 12$$

Where q_t, q_e and t are as defined above, and k_2 (g mg^{-1} min^{-1}) is the rate constant for the kinetic model. This model assumes that the rate of adsorption is controlled by the sharing of electrons between the adsorbent and adsorbate, i.e. a chemical process.

The overall kinetics of an adsorption process, when controlled by intra-particle diffusion [54],can be expressed by:

$$q_t = k_{id} t^{0.5} + q_e \qquad 13$$

Where q_t, q_e and t are as defined above, and k_{id} (mg $g^{-1}min^{1/2}$) is the intra-particle diffusion rate constant. Previous studies report that a plot of q_t vs. $t^{1/2}$ gives multi-linear steps controlled by the adsorption process[55, 56]. The initial portion is curved and due to bulk diffusion, followed by a linear portion attributed to intra-particle diffusion and, finally, a plateau, which results from equilibrium.

Table 5 shows the values obtained for each kinetic model obtained in this work, with the correspondingχ^2, R^2, and Δq % values. It is evident that the best fits, as denoted by the highest R^2 and lowest Δq% values, were obtained for the pseudo-second-order kinetic model (Figure9), suggesting chemical control of the adsorption process and the intra-particle diffusion model. Overall, the results obtained from the three kinetic models show that the adsorption kinetic models can be ordered: intra-particle> pseudo-second-order> pseudo-first-order forth equality

of fit that they provide for the adsorption of Cd (II) ions onto AAFW. This indicates that there is a combination of diffusional processes and surface chemical interactions that control the adsorption process studied here.

Mechanism of Adsorption

Given the low surface area of AAFW, in contrast with the high uptake of Cd(II) ions, it is evident that the high adsorption capacity of AAFW is independent of surface area and is, therefore, likely related to the high density of active surface functional groups. The results obtained for the kinetic modelling also indicate that some chemical interactions are involved in this adsorption process. Similar studies on relatively high metal adsorption on low specific surface area adsorbents have been reported in the literature [57, 58] and support the observations made here. The results obtained suggest that the removal of Cd (II) ions from aqueous solution onto the surface of AAFW may occur via a two steps, one physical and the other chemical. Firstly, the metal ions must diffuse to the surface of the sorbent, which involves migration of the sorptive from the bulk of the solution to the sorbent particles, (b) dispersion of the sorptive through the boundary layer to the external surface of the adsorbent, (c) adsorption at the dynamic sites on the external surface of AAFW, and finally (d) intra-particle-diffusion of the Cd(II) particles into the internal pores of the sorbent. In tandem, it is proposed that the metal ions chelate to

the sorbent via electron-donation from the combination of oxygen-and nitrogen-containing groups in AAFW to the electron-accepting Cd(II) ions (Scheme2).

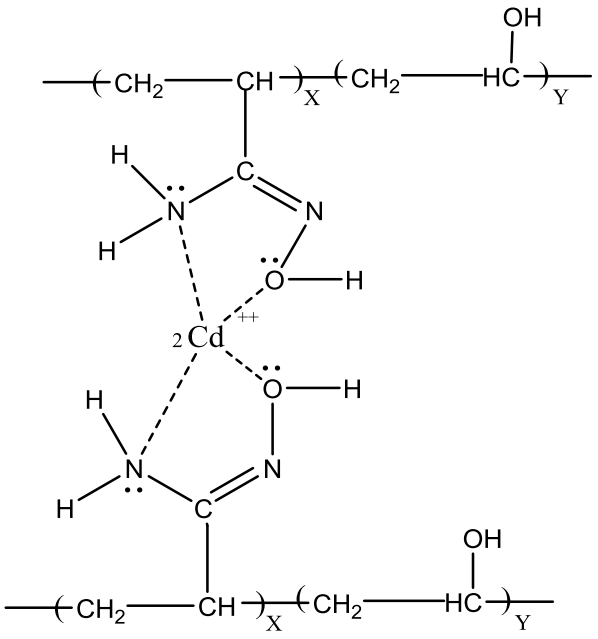

Scheme2: Schematic presentation of proposed complex structure between AAFW and Cd(II) ions.

4. Conclusions

The acrylic fiber waste was modified with hydroxylamine hydrochloride in alkaline medium to aminated acrylic fiber wastes (AAFW). The AAFW samples

were characterized by FT-IR spectral analysis, BET surface area, and SEM before and after adsorption of Cd(II). The AAFW were utilized for the extraction of Cd(II) ions from aqueous solution by using batch adsorption technique. The results indicated that the adsorption capacity of AAFW towards Cd(II) ions was affected by the contact time, adsorbent dose, pH and adsorbate concentration. Isothermal analysis showed that the Langmuir model provided the best fit of the experimental data, with a maximum predicted adsorption capacity of 253 mg g^{-1} at 30 °C. Adsorption was shown to be a favorable process and the kinetics of adsorption, obeying intra-particle diffusion and pseudo-second order models suggest overall chemical control of the adsorption process, possibly via a combination of physisorption, and complexation. Consequently, these aminated fiber wastes have been shown to be effective sorbents for the removal of Cd (II) ions from aqueous solution, demonstrating their potential role in water remediation processes.

References

1. Meena, A. K., K. Kadirvelu, G. K.Mishra, C.Rajagopal, P. N.Nagar,Adsorptive removal of heavy metals from aqueous solution by treated sawdust (Acacia arabica). Journal of hazardous materials, 2008. 150(3): p. 604-611.

2. Moulick, D., S.C. Santra, and D. Ghosh, Effect of selenium induced seed priming on arsenic accumulation in rice plant and subsequent transmission in human food chain. Ecotoxicology and environmental safety, 2018. 152: p. 67-77.

3. Meseguer V.F, J. F. Ortuño , M.I...Aguilar, M.L. Pinzón-Bedoya , M. Lloréns , J. Sáez , A. B. Pérez-Marín, Biosorption of cadmium (II) from aqueous solutions by natural and modified non-living leaves of Posidonia oceanica. Environmental Science and Pollution Research, 2016. 23(23): p. 24032-24046.

4. Ghodbane I. , L. Nouri, O. Hamdaoui, M. Chiha, Kinetic and equilibrium study for the sorption of cadmium (II) ions from aqueous phase by eucalyptus bark. Journal of Hazardous Materials, 2008. 152(1): p. 148-158.

5. Usman A., A. Sallam, M. Zhang, M. Vithanage, M. Ahmad, A. Al-Farraj, Y. S. Ok, A. Abduljabbar, M. Al-Wabel, Sorption process of date palm biochar for aqueous Cd (II) removal: Efficiency and mechanisms. Water, Air, & Soil Pollution, 2016. 227(12): p. 449.

6. Waalkes, M.P., Cadmium carcinogenesis in review. Journal of inorganic biochemistry, 2000. 79(1-4): p. 241-244.

7. A. Singh and S. M. Prasad, Remediation of heavy metal contaminated ecosystem: an overview on technology advancement, Int. J. Environ. Sci. Technol. 2015, 12:353–366.

8. Zhang,S., C. Yu, N. Liu, Y. Teng, C. Yin,Preparation of transparent anti-pollution cellulose carbamate regenerated cellulose membrane with high separation ability. International journal of biological macromolecules, 2019. 139: p. 332-341.

9. Gulgonul, I. and M.S. Çelik, Understanding the flotation separation of Na and K feldspars in the presence of KCl through ion exchange and ion adsorption. Minerals Engineering, 2018. 129: p. 41-46.

10. Li,M. , X. Xia, Z. Nie, L. Ma, Q. Liu, Recovery of tungsten from WC–Co hard metal scraps using molten salts electrolysis. Journal of Materials Research and Technology, 2019. 8(1): p. 1440-1450.

11. Wang,T., Q. Wang, H. Soklun, G. Qu, T. Xia, X. Guo, H. Jia, L. Zhu, A green strategy for simultaneous Cu (II)-EDTA decomplexation and Cu precipitation from water by

497 bicarbonate-activated hydrogen peroxide/chemical precipitation. Chemical Engineering
498 Journal, 2019. 370: p. 1298-1309.
499 12. Hasanzadeh, V., O. Rahmanian, and M. Heidari, Cefixime adsorption onto activated carbon
500 prepared by dry thermochemical activation of date fruit residues. Microchemical Journal,
501 2020. 152: p. 104261.
502
503 13.Ma, Liang, M. He, P. Fu, X. Jiang, W. Lv, Y. Huang, Y. Liu, H. Wang, Adsorption of volatile
504 organic compounds on modified spherical activated carbon in a new cyclonic fluidized bed.
505 Separation and Purification Technology, 2020. 235: p. 116146.
506 14.Hashem A. ,H. A. Hussein,M. A. Sanousy,E. Adam and E. E. Saad,, Monomethylolated
507 thiourea–sawdust as a new adsorbent for removal of Hg (II) from contaminated water:
508 equilibrium kinetic and thermodynamic studies. Polymer-Plastics Technology and
509 Engineering, 2011. 50(12): p. 1220-1230.
510 15. Hashem, A. and S.M. Badawy, Sesbania sesban L. biomass as a novel adsorbent for removal
511 of Pb (II) ions from aqueous solution: non-linear and error analysis. Green Processing and
512 Synthesis, 2015. 4(3): p. 179-190.
513 16. Kwon J-S , S-T Yun, J-H. Lee, S-O Kim, H Y Jo, Removal of divalent heavy metals (Cd,
514 Cu, Pb, and Zn) and arsenic (III) from aqueous solutions using scoria: kinetics and equilibria
515 of sorption. Journal of Hazardous Materials, 2010. 174(1-3): p. 307-313.
516 17. Hashem, A., H.A. Hammad, and A. Al-Anwar, Modified Camelorum tree particles as a new
517 adsorbent for adsorption of Hg (II) from aqueous solutions: kinetics, thermodynamics and
518 non-linear isotherms. Desalination and Water Treatment, 2016. 57(50): p. 23827-23843.
519 18.Hashem, A., A. Al-Anwar, N. M. Nagy, D. M. Hussein, S. M Eisa. Isotherms and kinetic
520 studies on adsorption of Hg (II) ions onto Ziziphus spina-christi L. from aqueous solutions.
521 Green Processing and Synthesis, 2016. 5(2): p. 213-224.
522 19. Wu,Y., Y. Fan, M. Zhang, Z. Ming, S. Yang, A. Arkin, P. Fang, Functionalized agricultural
523 biomass as a low-cost adsorbent: Utilization of rice straw incorporated with amine groups
524 for the adsorption of Cr (VI) and Ni (II) from single and binary systems. Biochemical
525 Engineering Journal, 2016. 105: p. 27-35.
526 20. Xu,C., J. Wang , T. Yang , X. Chen , X. Liu , X. Ding,

Adsorption of uranium by amidoximated chitosan-grafted polyacrylonitrile, using response surface methodology. Carbohydrate polymers, 2015. 121: p. 79-85.

21.Abdouss,M., A. M. Shoushtari, N. Shamloo, A. Haji,

Modified PET fibres for metal ion and dye removal from aqueous media. Polymers and Polymer Composites, 2013. 21(4): p. 251-258.

22. Racho, P. and P. Phalathip, Modified nylon fibers with amino chelating groups for heavy metal removal. Energy Procedia, 2017. 118: p. 195-200.

23. Abdouss, M., A. Mousavi, Shoushtari, A. Haji, B. Moshref, Fabrication of chelating diethylenetriaminated pan micro-and nano-fibers for heavy metal removal. Chemical Industry and Chemical Engineering Quarterly/CICEQ, 2012. 18(1): p. 27-34.

24. Rangabhashiyam S., N. Anu, M.S. Giri Nandagopal, N. Selvaraju, Relevance of isotherm models in biosorption of pollutants by agricultural byproducts. Journal of Environmental Chemical Engineering, 2014. 2(1): p. 398-414.

25. Ng, J., W. Cheung, and G. McKay, Equilibrium studies of the sorption of Cu (II) ions onto chitosan. Journal of Colloid and Interface Science, 2002. 255(1): p. 64-74.

26. Karaca S. A. Gürses, M. Ejder, M. Açikyildiz, Kinetic modeling of liquid-phase adsorption of phosphate on dolomite. Journal of Colloid and Interface Science, 2004. 277(2): p. 257-263..

27. Kapoor, A. and R. Yang, Correlation of equilibrium adsorption data of condensible vapours on porous adsorbents. Gas Separation & Purification, 1989. 3(4): p. 187-192.

28. Hossain, M., H. Ngo, and W. Guo, Introductory of Microsoft Excel SOLVER function-spreadsheet method for isotherm and kinetics modelling of metals biosorption in water and wastewater. Journal of Water Sustainability, 2013.

29. A. Hashem, S.M. Badawy, S. Faraga, L.A. Mohamed, A.J. Fletcher, G.M. Tahaa, Non-linear adsorption characteristics of modified pine wood sawdust optimised for adsorption of Cd(II) from aqueous systems, Journal of Environmental Chemical, Engineering, 2020.8: 103966.

30. Sing, K.S., Reporting physisorption data for gas/solid systems with special reference to the determination of surface area and porosity (Provisional). Pure and applied chemistry, 1982. 54(11): p. 2201-2218.

31.Thommes,M., K. Kaneko, A. V. Neimark, J. P. Olivier,F. R-Reinoso, J. Rouquerol and K. S. W. Sing, Physisorption of gases, with special reference to the evaluation of surface area and

pore size distribution (IUPAC Technical Report). Pure and Applied Chemistry, 2015. 87(9-10): p. 1051-1069.

32. Martín-Lara M. Á. , F. Hernáinz, M. Calero, G. Blázquez, G. Tenorio, Surface chemistry evaluation of some solid wastes from olive-oil industry used for lead removal from aqueous solutions. Biochemical Engineering Journal, 2009. 44(2-3): p. 151-159.
33. Khalil, A., H. H.Sokker, A.Al-Anwar and A. Hashem., Preparation, Characterization and Utilization of Amidoximated Poly (AN/MAA)-grafted Alhagi Residues for the Removal of Zn (II) Ions from Aqueous Solution. Adsorption Science & Technology, 2009. 27(4): p. 363-382.
34. Chen, H., Y. Zhao, and A. Wang, Removal of Cu (II) from aqueous solution by adsorption onto acid-activated palygorskite. Journal of Hazardous Materials, 2007. 149(2): p. 346-354.
35. Azouaou N., Z. Sadaoui, A. Djaafri, H. Mokaddem, Adsorption of cadmium from aqueous solution onto untreated coffee grounds: Equilibrium, kinetics and thermodynamics. Journal of hazardous materials, 2010. 184(1-3): p. 126-134.
36. Balkaya, N. and H. Cesur, Adsorption of cadmium from aqueous solution by phosphogypsum. Chemical engineering journal, 2008. 140(1-3): p. 247-254.
37. Patterer M. S. , I. Bavasso, J. E. Sambeth, F. Medici, Cadmium removal from acqueous solution by adsorption on spent coffee grounds. 2017.
38. Ma, F., B. Zhao, and J. Diao, Adsorption of cadmium by biochar produced from pyrolysis of corn stalk in aqueous solution. Water Science and Technology, 2016. 74(6): p. 1335-1345.
39. Masoudi R. , H. Moghimi ,E. Azin & R. A. Taheri, Adsorption of cadmium from aqueous solutions by novel Fe3O4-newly isolated Actinomucor sp. bio-nanoadsorbent: functional group study. Artificial cells, nanomedicine, and biotechnology, 2018. 46(sup3): p. S1092-S1101.
40. Al-Anber, Z.A. and M.A.D. Matouq, Batch adsorption of cadmium ions from aqueous solution by means of olive cake. Journal of hazardous materials, 2008. 151(1): p. 194-201.
41. Hasan S. , A. Krishnaiah, T. K. Ghosh, D. S. Viswanath, V. M. Boddu, and E. D. Smith, Adsorption of divalent cadmium (Cd (II)) from aqueous solutions onto chitosan-coated perlite beads. Industrial & engineering chemistry research, 2006. 45(14): p. 5066-5077.

42. Wang, F.Y., H. Wang, and J.W. Ma, Adsorption of cadmium (II) ions from aqueous solution by a new low-cost adsorbent—Bamboo charcoal. Journal of hazardous materials, 2010. 177(1-3): p. 300-306.
43. Tajar, A.F., T. Kaghazchi, and M. Soleimani, Adsorption of cadmium from aqueous solutions on sulfurized activated carbon prepared from nut shells. Journal of Hazardous Materials, 2009. 165(1-3): p. 1159-1164.
44. Langmuir, I., The constitution and fundamental properties of solids and liquids. Part I. Solids. Journal of the American chemical society, 1916. 38(11): p. 2221-2295.
45. Hall K. R. , L. C. Eagleton, A. Acrivos , and T. Vermeulen, Pore-and solid-diffusion kinetics in fixed-bed adsorption under constant-pattern conditions. Industrial & Engineering Chemistry Fundamentals, 1966. 5(2): p. 212-223.
46. Freundlich, H., Über die adsorption in lösungen. Zeitschrift für physikalische Chemie, 1907. 57(1): p. 385-470.
47. Temkin, M., Kinetics of ammonia synthesis on promoted iron catalysts. Acta physiochim. URSS, 1940. 12: p. 327-356.
48. Redlich, O. and D.L. Peterson, A useful adsorption isotherm. Journal of Physical Chemistry, 1959. 63(6): p. 1024-1024.
49. Toth, J., State equation of the solid-gas interface layers. Acta chim. hung., 1971. 69: p. 311-328.
50. Sips, R., On the structure of a catalyst surface. The Journal of Chemical Physics, 1948. 16(5): p. 490-495.
51. Khan, A., R. Ataullah, and A. Al-Haddad, Equilibrium adsorption studies of some aromatic pollutants from dilute aqueous solutions on activated carbon at different temperatures. Journal of colloid and interface science, 1997. 194(1): p. 154-165.
52. Lagergren, S.K., About the theory of so-called adsorption of soluble substances. Sven. Vetenskapsakad. Handingarl, 1898. 24: p. 1-39.
53. Ho, Y.-S. and G. McKay, Pseudo-second order model for sorption processes. Process biochemistry, 1999. 34(5): p. 451-465.
54. Weber, W.J. and J.C. Morris, Kinetics of adsorption on carbon from solution. Journal of the Sanitary Engineering Division, 1963. 89(2): p. 31-60.

55. Unuabonah, E., K. Adebowale, and B. Olu-Owolabi, Kinetic and thermodynamic studies of the adsorption of lead (II) ions onto phosphate-modified kaolinite clay. Journal of Hazardous Materials, 2007. 144(1-2): p. 386-395.
56. Boparai, H.K., M. Joseph, and D.M. O'Carroll, Kinetics and thermodynamics of cadmium ion removal by adsorption onto nano zerovalent iron particles. Journal of hazardous materials, 2011. 186(1): p. 458-465.
57. Qi L., F. Teng, X. Deng , Y. Zhang, X. Zhong, Experimental study on adsorption of Hg (II) with microwave-assisted alkali-modified fly ash. Powder Technology, 2019. 351: p. 153-158.
58. Hu, M., H. Tian, and J. He, Unprecedented Selectivity and Rapid Uptake of CuS Nanostructures toward Hg (II) Ions. ACS applied materials & interfaces, 2019.

628 **List of Tables**

629

630 **Table 3**: Isotherm constants of two-parameter isotherm models applied to experimental data
631 obtained for Cd(II) ions adsorption onto AAFW at 30 °C.
632

Isotherm Model	Parameter	Value	Error Analysis	Value
Langmuir	a_L	0.0019	ARE	0.3083
	k_L	1.779	APE %	4.4043
	Q_{max}	252.842	Hybrid	5.813
			χ^2	5.103
			R^2	0.9984
Freundlich	n	1.762	ARE	0.797
	K_F	13.0140	APE %	11.379
			Hybrid	34.042
			χ^2	24.765
			R^2	0.9871
Temkin	A_T	67.271	ARE	4.352
	b_T	60	APE %	62.176
			Hybrid	868.967
			χ^2	385.766
			R^2	0.974

633
634

635 **Table 4**: Isotherm constants of three-parameter models applied to experimental data obtained for
636 Cd(II) ions adsorption onto AAFW at 30 °C.
637

Isotherm Model	Parameter	Value	Error Analysis	Value
Redlich -Peterson	kg	10.209	ARE	1.417
	α_R	-0.875	APE %	20.241
	g	0.0171	Hybrid	105.457
			χ^2	65.388
			R^2	0.933
Sips	K_S	1.581	ARE	0.252
	α_S	0.0016	APE %	3.606
	βS	1.014	Hybrid	2.949
			χ^2	2.729
			R^2	0.998
Toth	k_T	13.021	ARE	0.796
	α_T	0.0901	APE %	11.372
	1/t	0.432	Hybrid	33.995
			χ^2	24.737
			R^2	0.987
Khan	q_m	0.662	ARE	0.684
	b_K	89.070	APE %	9.777
			Hybrid	20.921
			χ^2	16.912
			R^2	0.984
	α_K	0.393		

638

639 **Table 5**: Constants of kinetic models applied to experimental data obtained for Cd(II) ions
640 adsorption onto AAFW at 30 °C
641

Isotherm Model	Parameter	Value	Error Analysis	Value
Pseudo First-Order	q_e	88.496	ARE	1.065
	k_1	0.036	APE %	13.311
			Hybrid	20.579
			R^2	0.980
			Δq(%)	22.652
Pseudo Second-Order	q_e	94.209	ARE	0.629
	k_2	0.0008	APE %	7.871
			Hybrid	6.889
			R^2	0.993
			Δq(%)	13.25
Intra-Particle	k_{id}	4.086		0.479
	C	34.702	ARE	5.994
			APE %	2.886
			Hybrid	0.994
			R^2	2.408
			Δq(%)	

642

643 **List of Figures**

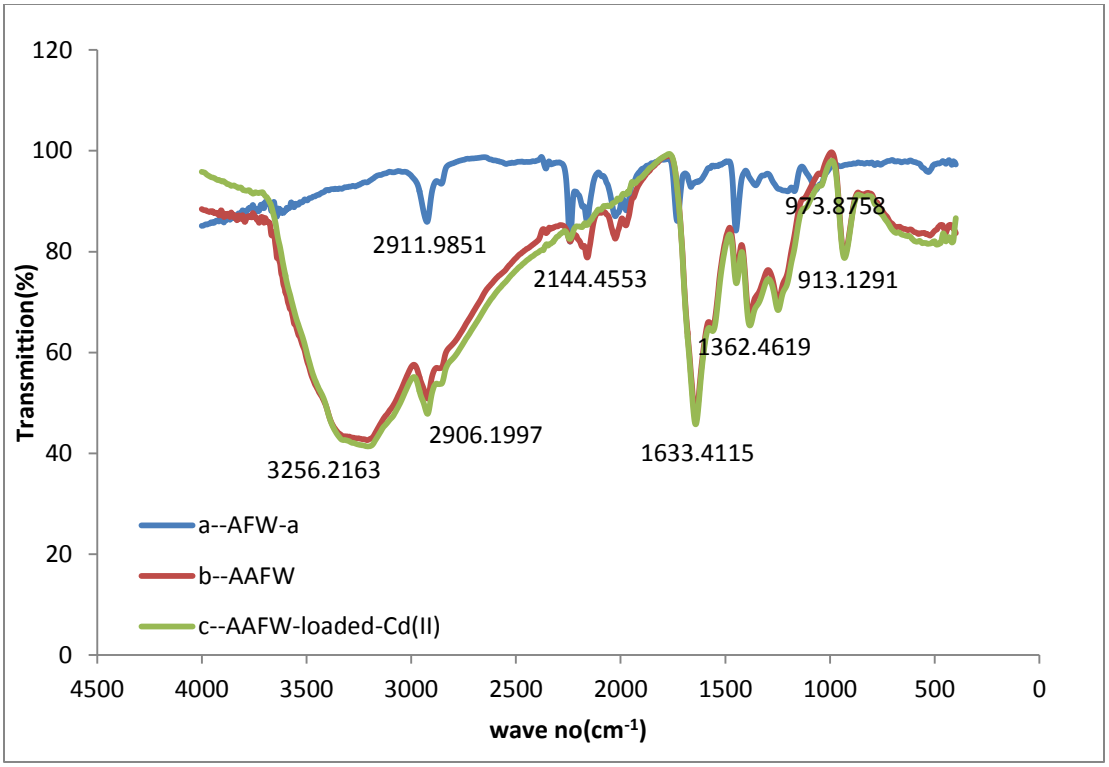

644

645 **Fig.1**: FT-IR of (a) acrylic fiber waste (AFW), (b) aminated acrylic fiber waste (AAFW) and (c)
646 AAFW-loaded with Cd(II) ions.

647

648

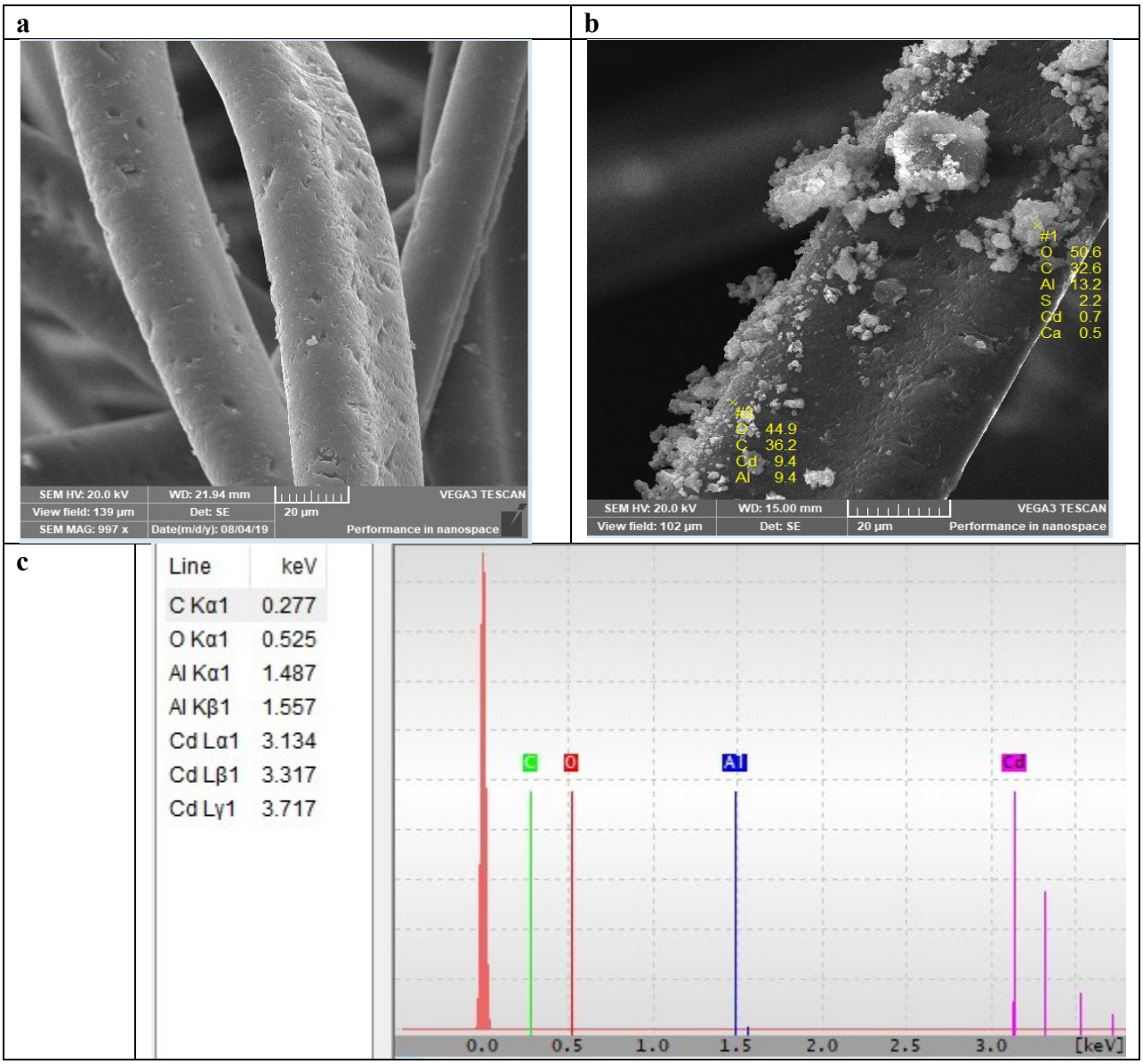

Fig. 2: Scanning electron micrographs of (a) AAFW, (b) AAFW loaded with Cd(II) ions, and (c) EDX of AAFW loaded with Cd(II) ions(c).

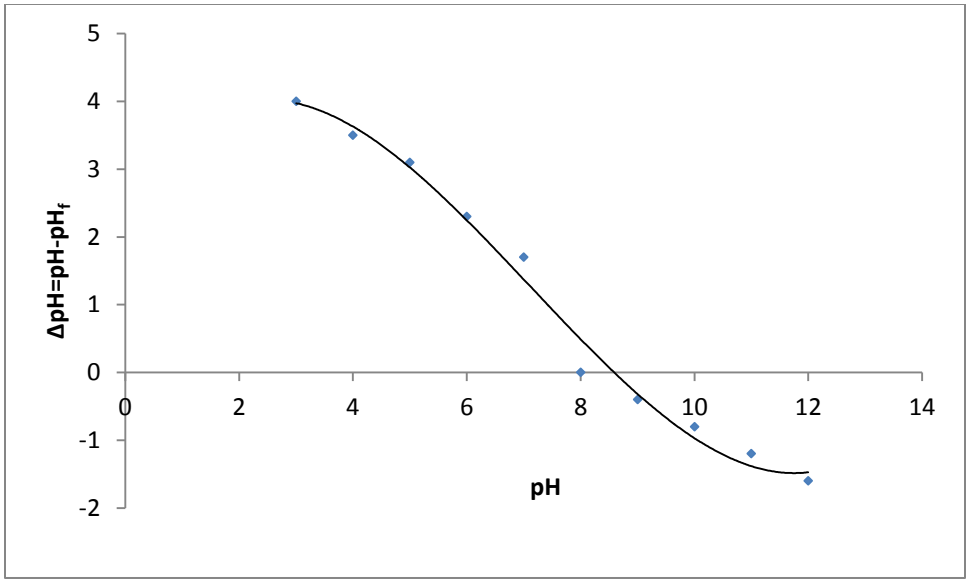

Fig. 3: pH measurements to determine the point of zero charge for AAFW surface.

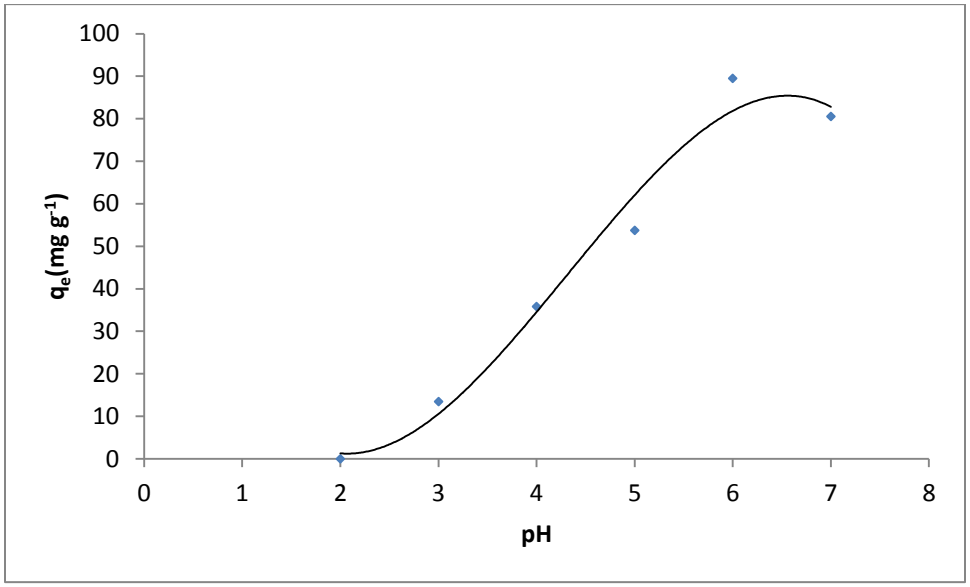

Fig. 4: Effect of pH on adsorption capacity of Cd(II) ions onto AAFW at 30 °C. Reaction conditions: Cd(II) ion concentration: 300 mg L^{-1}; adsorbent concentration: 0.3 g L^{-1}; contact time: 2 h.

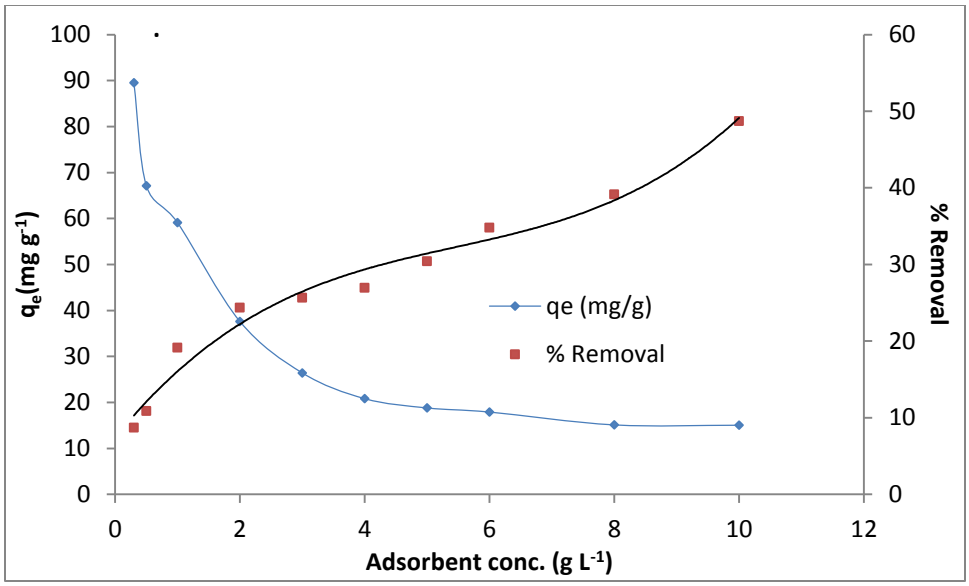

664

665 **Fig. 5**: Effect of adsorbent concentration on both adsorption capacity and % removal of Cd(II)
666 ions onto AAFW at 30 °C. Reaction conditions: Cd(II) ion concentration: 300 mg L^{-1}; pH 6;
667 contact time: 2 h.
668
669
670

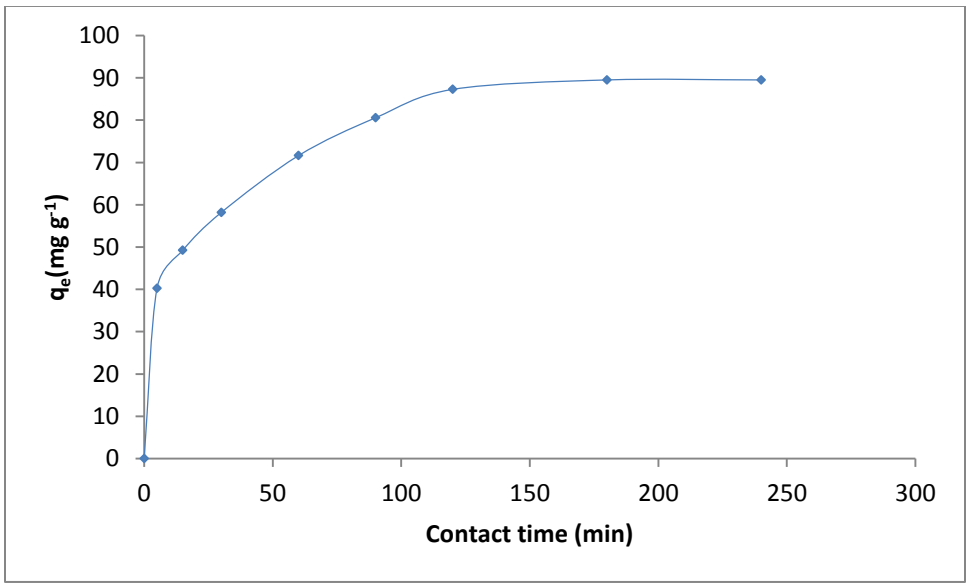

671

672 **Fig. 6**: Effect of contact time on adsorption capacity of Cd(II) ions onto AAFW sorbent at 30 °C.
673 Reaction conditions: Cd(II) ion concentration: 300 mg L^{-1}; adsorbent concentration: 0.5 g L^{-1}; pH
674 6.

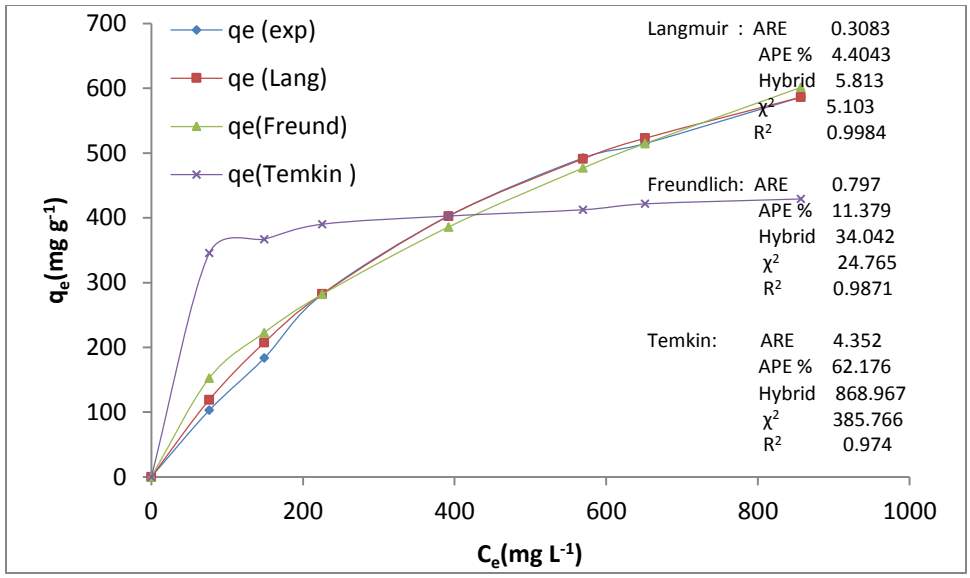

675

676 **Fig. 7**: Comparison between two-parameter isotherm models and experimental data obtained for
677 adsorption on Cd(II) ions onto AAFW at 30 °C. Reaction conditions: Cd(II) ion concentration:
678 300 mg L^{-1}; adsorbent concentration: 0.5 g L^{-1}; pH 6.

679

680

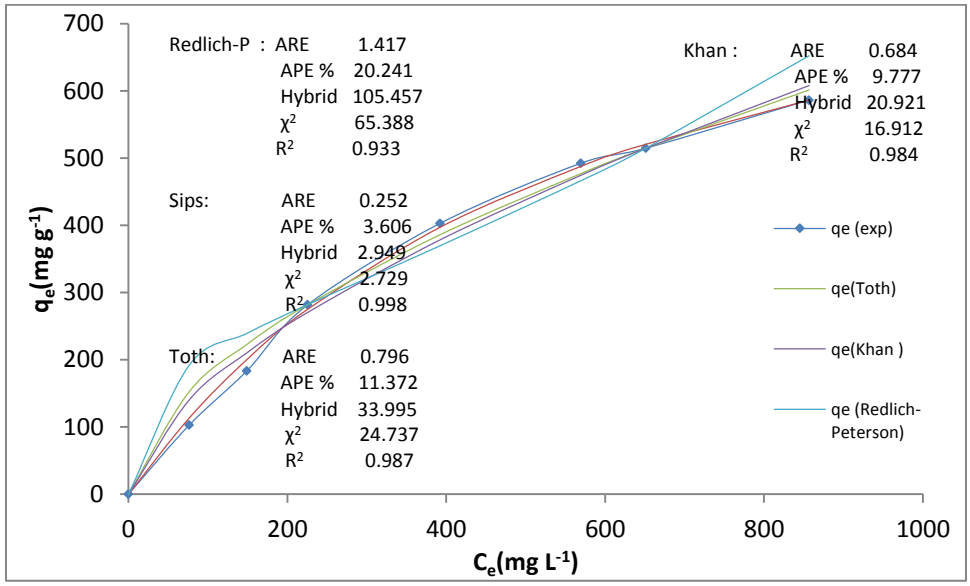

681

682 **Fig. 8**: Comparison between three-parameter isotherm models and experimental data obtained
683 for adsorption on Cd(II) ions onto AAFW at 30 °C. Reaction conditions: Cd(II) ion
684 concentration: 300 mg L^{-1}; adsorbent concentration: 0.5 g L^{-1}; pH 6.

685

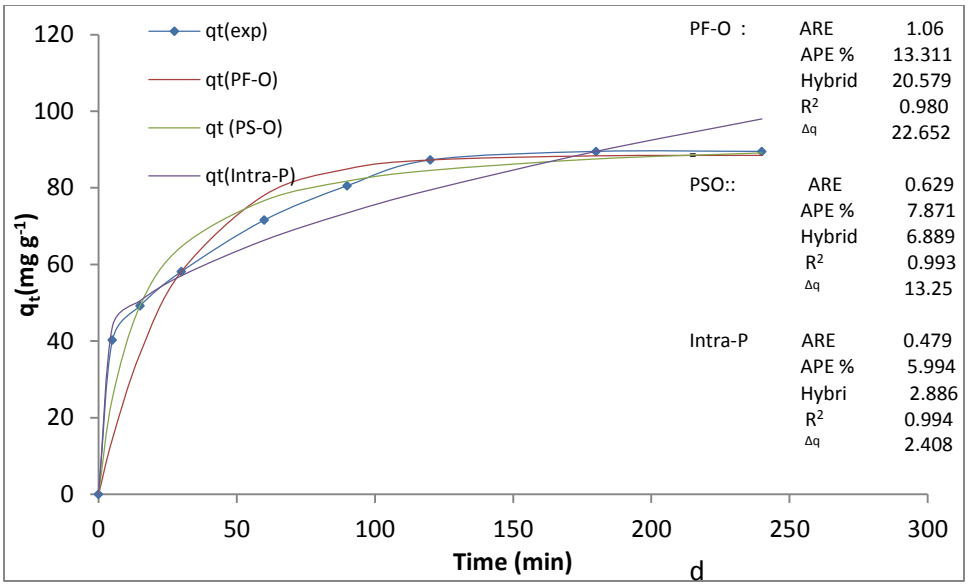

686 d

687 **Fig. 9**: Comparison between selected kinetic models and experimental data obtained for
688 adsorption on Cd(II) ions onto AAFW at 30 °C. Reaction conditions: Cd(II) ion concentration:
689 300 mg L^{-1}; adsorbent concentration: 0.5 g L^{-1}; pH 6.

690